JOURNAL OF GUIDANCE, CONTROL, AND DYNAMICS
Vol. 18, No. 6, November–December 1995

Analytical Models of Doppler Data Signatures

Connie J. Weeks* and Melissa J. Bowers†
Loyola Marymount University, Los Angeles, California 90045

A primary indicator of the accuracy of orbit determination based on Doppler tracking is the graph of residuals vs time. Parameter errors in the orbit determination model produce characteristic signatures in the residuals plot. A systematic method of modeling the signature due to a parameter error by means of first and second partial derivative approximations is presented. Signatures due to errors in station location, solar pressure, relativistic clock, and the Earth's troposphere are compared with residual plots from a spacecraft mission, corresponding to the introduction of the same parametric error into orbit determination software. A comparison of postfit residuals with and without the introduction of known modeling errors demonstrates that some errors can be masked by apparent convergence, resulting in erroneous estimates.

Introduction

DOPPLER tracking is a radiometric data type that provides a measure of the component of velocity along the line of sight between a tracking station and a spacecraft by the deep space network. Doppler is the primary data type used to determine the orbit of the spacecraft. The Doppler measurement Z_m is a count of the difference between the number of cycles transmitted and received by a ground station, divided by the count time. Accurate orbit determination depends not only on accurate models of spacecraft dynamics and gravitational forces but also on models of errors due to transmission media and instrumentation. Whereas models of errors due to transmission media, Earth platform parameters, and relativistic time keeping are known, in practice some parameters in the models are not well determined, and errors from these sources cannot be entirely removed from the data.

A primary indicator of the accuracy of estimates is the graph of residuals vs time. The term residual refers to the difference between a measured value and the computed value based on a model or estimate. Parameter errors in an orbit determination model produce characteristic signatures or shapes in the residuals plot. A method of modeling a signature in the residuals, which may provide a useful diagnostic tool, is developed using first- and second-order partial derivative approximations. To illustrate the method, signature models due to parameter errors in station location, solar pressure, relativistic clock, and the Earth's troposphere are compared with residual plots from a spacecraft mission, corresponding to the introduction of the same parametric errors into the orbit determination model.

The analysis used here was first proposed by Miller[1] but was used only to obtain bounds on error sensitivity. The physical models are essentially the same as those contained in the Jet Propulsion Laboratory orbit determination program.[2]

Analysis

The Doppler measurement, in hertz, is a measure of phase change over time,

$$Z_m = \frac{N_r - N_c}{\Delta T_c} + \text{noise} \tag{1}$$

where N_c is the number of cycles transmitted and N_r is the number of cycles received over some time interval ΔT_c. The noise, due primarily to instrumentation error, is typically about 0.1 cycle.

Figure 1 illustrates the Earth station–spacecraft–Earth station Doppler signal path. Subscripts $1s$ and $1e$ refer to the beginning and end of transmission time at the station, $2s$ and $2e$ the beginning and end of returning transmissions from the spacecraft, and $3s$ and $3e$ the received transmission times at the station. The relevant light path distances in between are given by ρ_{ij}. ΔT_{rtlt} refers to the round trip light time.

From Fig. 1 we have the following expressions for N_c, N_r, and ΔT_c:

$$\begin{aligned} N_c &= C_3 f_t (T_{3e} - T_{3s}) \\ N_r &= C_3 f_t (T_{1e} - T_{1s}) \\ \Delta T_c &= T_{3e} - T_{3s} \end{aligned} \tag{2}$$

The constant C_3 is the spacecraft turnaround ratio, which for X-band Doppler is 880/749, and f_t is the frequency of the signal transmitted by the station, which for X-band Doppler is 7.17×10^9 Hz.

Thus, the Doppler measurement is given by

$$Z_m = (C_3 f_t / \Delta T_c)[(T_{3e} - T_{3s}) - (T_{1e} - T_{1s})] \tag{3}$$

where T represents station time. If t represents spacecraft ephemeris time, and $F(t, X, Y)$ is a calibration function representing differences between the station time T and the spacecraft ephemeris time t, due to relativity and other parameters, we have

$$T = t + F(t, X, Y) \tag{4}$$

where the vectors $\boldsymbol{X}$ and $\boldsymbol{Y}$ represent the state and a vector of constant parameters, respectively. Thus

$$T_3 - T_1 = t_3 - t_1 + F(t_3, X, Y) - F(t_1, X, Y) \tag{5}$$

The difference in sent and received times is a function of the time it takes to travel from Earth station to spacecraft to Earth, plus media

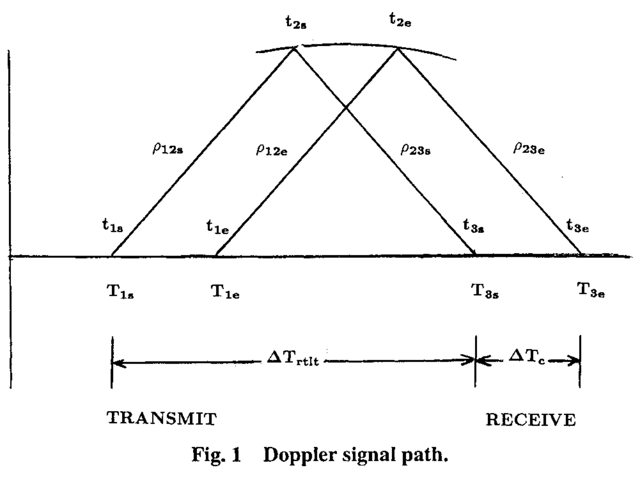

Fig. 1 Doppler signal path.

Received June 6, 1994; revision received Jan. 30, 1995; accepted for publication June 1, 1995.

*Associate Professor, Department of Mathematics.
†Senior Mathematics Major, Department of Mathematics.

delays, such as tropospheric distortion at the beginning and end of each trip. If $G(t, \boldsymbol{X}, \boldsymbol{Y})$ represents media delays,

$$t_3 - t_1 = \frac{\rho_{12} + \rho_{23}}{c} + G(t_1, \boldsymbol{X}, \boldsymbol{Y}) + G(t_3, \boldsymbol{X}, \boldsymbol{Y}) \tag{6}$$

The computed Doppler measurement is given by

$$\begin{aligned} Z_c = {} & \frac{C_3 f_t}{\Delta T_c}[(T_{3e} - T_{1e}) - (T_{3s} - T_{1s})] \\ = {} & \frac{C_3 f_t}{\Delta T_c}[(t_{3e} - t_{1e}) - (t_{3s} - t_{1s}) + F(t_{3e}) \\ & - F(t_{1e}) - F(t_{3s}) + F(t_{1s})] \\ = {} & \frac{C_3 f_t}{\Delta T_c}\frac{\rho_{12e} + \rho_{23e} - \rho_{12s} - \rho_{23s}}{c} \\ & + \frac{C_3 f_t}{\Delta T_c}[G(t_{3e}, \boldsymbol{X}, \boldsymbol{Y}) - G(t_{3s}, \boldsymbol{X}, \boldsymbol{Y}) \\ & + G(t_{1e}, \boldsymbol{X}, \boldsymbol{Y}) - G(t_{1s}, \boldsymbol{X}, \boldsymbol{Y})] \\ & + \frac{C_3 f_t}{\Delta T_c}[F(t_{3e}, \boldsymbol{X}, \boldsymbol{Y}) - F(t_{3s}, \boldsymbol{X}, \boldsymbol{Y}) \\ & - F(t_{1e}, \boldsymbol{X}, \boldsymbol{Y}) + F(t_{1s}, \boldsymbol{X}, \boldsymbol{Y})] \end{aligned} \tag{7}$$

The range and media portions of Eq. (7) may be approximated by first-order differentials

$$\begin{aligned} \frac{\rho_{12e} - \rho_{12s}}{c} &\approx \dot{\rho}\Delta T_c \\ \frac{\rho_{23e} - \rho_{23s}}{c} &\approx \dot{\rho}\Delta T_c \end{aligned} \tag{8}$$

Here $\dot{\rho}$ is the time derivative of the range function $\rho(t, \boldsymbol{X}, \boldsymbol{Y})$ obtained by integrating the equations of motion. Similarly,

$$\begin{aligned} G(t_{1e}) - G(t_{1s}) &\approx \frac{\partial G}{\partial t}\Delta T_c \\ G(t_{3e}) - G(t_{3s}) &\approx \frac{\partial G}{\partial t}\Delta T_c \end{aligned} \tag{9}$$

Contributions in opposite directions due to clock calibration have opposite signs. Thus, the clock calibration portion of Eq. (7) represents a difference of a difference and is best approximated by a second-order differential. The following definition is applied:

$$\frac{\partial^2 F}{\partial t^2} = \lim_{\Delta t_2 \to 0} \lim_{\Delta t_1 \to 0} \times \frac{[F(t + \Delta t_1 + \Delta t_2) - F(t + \Delta t_2)] - [F(t + \Delta t_1) - F(t)]}{\Delta t_1 \Delta t_2} \tag{10}$$

If $\Delta t_1 \approx \Delta T_c$ and $\Delta t_2 \approx \Delta t_{\mathrm{rtlt}}$, a second-order differential approximation for the clock calibration term is given by

$$F(t_{3e}) - F(t_{1e}) - F(t_{3s}) + F(t_{1s}) \approx \frac{\partial^2 F}{\partial t^2}\Delta T_c \Delta t_{\mathrm{rtlt}} \tag{11}$$

We have the following approximate formula for the Doppler data type:

$$Z_m \approx C_3 f_t\left[\frac{2\dot{\rho}}{c} + 2\frac{\partial G(t_{1e})}{\partial t} + \frac{\partial^2 F(t)}{\partial t^2}\Delta t_{\mathrm{rtlt}}\right] \tag{12}$$

The sensitivity of Z_m to a change in the $\boldsymbol{Y}$ parameter vector is given by

$$\Delta Z_m \approx C_3 f_t\left[2\frac{\partial^2 \rho(t, \boldsymbol{X}, \boldsymbol{Y})}{\partial \boldsymbol{Y}\partial t} + 2\frac{\partial^2 G(t, \boldsymbol{X}, \boldsymbol{Y})}{\partial \boldsymbol{Y}\partial t} + \frac{\partial^3 F(t, \boldsymbol{X}, \boldsymbol{Y})}{\partial \boldsymbol{Y}\partial t^2}\Delta t_{\mathrm{rtlt}}\right]\Delta \boldsymbol{Y} \tag{13}$$

When explicit functions for the range ρ and clock and media calibrations F and G are specified, this equation provides not only a ready numerical determination of sensitivity to parameter errors but also a time-dependent equation for recognizable signatures in residual plots due to specific parameter errors.

Results are illustrated for errors in relativistic clock, station location, solar pressure, and troposphere models. In each case, a parameter error is introduced into the orbit determination program. Residual plots are generated for 9000 s of data from the Mars Observer mission. The plot is then compared with the analytical model of the error signature from Eq. (13). Each day represents one pass from each of three Earth stations, at Goldstone, Madrid, and Canberra. Toward the latter part of the data, some passes are missing, because data was not taken continuously during that time period.

Solar Pressure Signature

As an example of a signature in the Doppler residuals plot, due to a modeling error, consider solar pressure. Solar pressure acting on the spacecraft applies an acceleration along the line of sight from Earth to spacecraft given by

$$a = (Ak/r^2 m)R\cos\theta \tag{14}$$

where

A = area of spacecraft, 3.879 m^2
k = solar constant (mixed units), 1.01×10^8
r = distance from sun to spacecraft, 1.872×10^8 km
m = mass of spacecraft, 341.214 kg
R = reflectivity constant, 1.011259
θ = Earth/spacecraft/sun angle, 24.4 deg

An error in the reflectivity constant ΔR will produce a constant acceleration error along the line of sight given by

$$\Delta a = \frac{\partial a}{\partial R}\Delta R = \frac{Ak}{r^2 m}(\Delta R)\cos\theta \tag{15}$$

The Doppler residual plot in Fig. 2 illustrates the signature corresponding to an error $\Delta R = 0.1$ in the form of a ramp, indicating the constant acceleration error. The slope of the ramp closely approximates the constant acceleration error Δa. The residual plot is in hertz vs time. Using 0.057 Hz = 1 mm/s for X-band Doppler, we have for the slope

$$\frac{5 \times 10^{-7}\ \mathrm{km/s}}{172800\ \mathrm{s}} = 2.89 \times 10^{-12}\ \mathrm{km/s}$$

The value calculated from (15) is 2.98×10^{-12} km/s.

In the following three examples, consider the Earth-centered inertial reference frame in Fig. 3. The spacecraft lies in the xz plane a distance r from the Earth. The direction of the spacecraft is given by the right ascension α and declination δ, respectively. A tracking station located on the Earth is at a radial distance r_s, with longitude λ_s and latitude ϕ_s. If ω_e is the Earth rotation rate, the angle λ between the x axis and the projection of the tracking station position vector onto the xy plane is given by

$$\lambda = \omega_e t + \lambda_s - \alpha \tag{16}$$

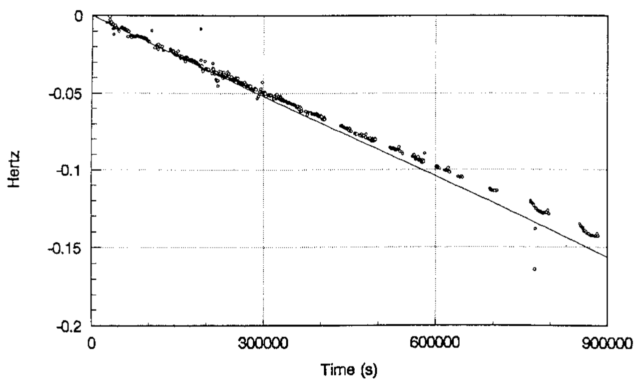

Fig. 2 Solar pressure residual plot with signature model.

Table 1 Tracking station locations

Station	Longitude, °	Latitude, °
Goldstone	243.1	35.23
Canberra	148.9	−35.21
Madrid	355.7	40.46

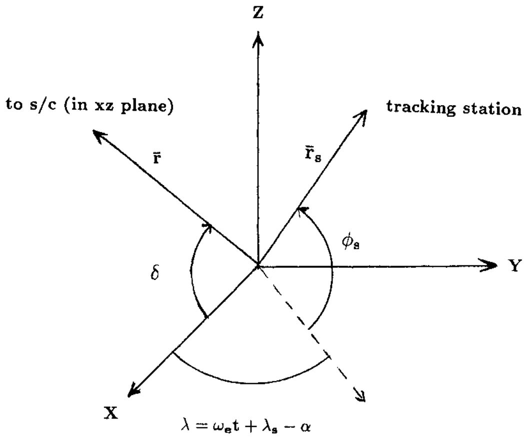

Fig. 3 Earth-centered inertial reference frame.

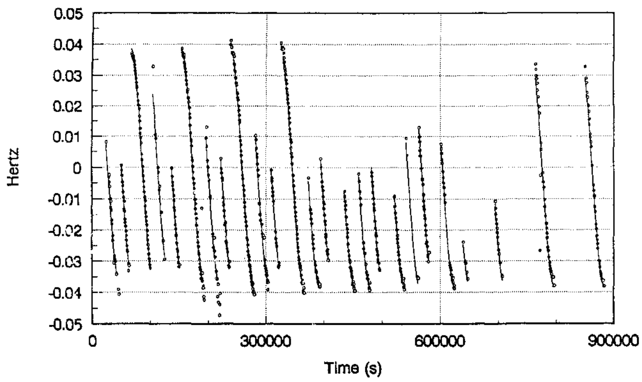

Fig. 4 Station location residuals with signature model.

For this study typical constants are Earth rotation rate $\omega_e = 7.272 \times 10^{-5}$ rad/s, tracking station radius $r_s = 5204$ km, and spacecraft declination $\delta = 17.46$ deg. The station longitudes and latitudes are listed in Table 1. The right ascension α of the spacecraft is included as part of a phase angle that is determined experimentally for each example.

Station Location Error Signature

The approximate variation in the range between the spacecraft and an Earth station due to the Earth rotation is given by[3]

$$R_s = (1/c) r_s \cos\delta \sin(\omega_e t + \lambda_s + \theta_{sl}) \tag{17}$$

where the function is premultiplied by $1/c$ to give it units of time consistent with other calibration functions, and θ_{sl} is a phase angle dependent on the inertial coordinate system (refer to Fig. 3). If an error is introduced in the spin radius r_s, from Eq. (13) we know the sensitivity to the error will be given by

$$\Delta Z = 2C_3 f_t \frac{\partial^2 R_s}{\partial r_s \partial t} \Delta r_s$$

$$= \frac{2C_3 f_t}{c} \omega_e \cos\delta \cos(\omega_e t + \lambda_s + \theta_{sl}) \Delta r_s \tag{18}$$

Figure 4 illustrates the Doppler residual plot for 9000 s, after an error of 0.01 km is introduced into the value for r_s. Three plots

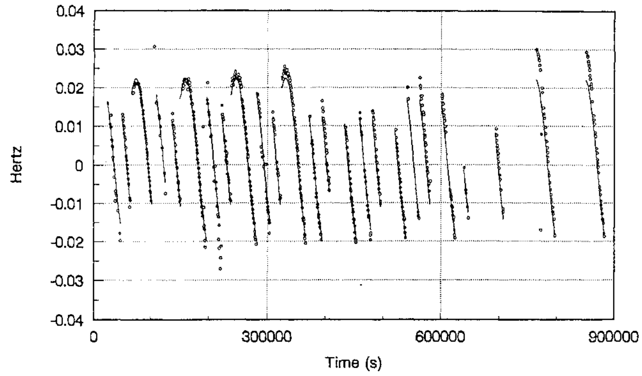

Fig. 5 Clock calibration residual with signature model.

of Eq. (18) are matched to each of the three stations, using the appropriate longitude λ_s for each station and a phase angle $\theta_{sl} = 90$ deg.

Relativistic Clock Error Signature

As an example of a signature model for an error in the calibration of the clock on an Earth station, consider the special relativity correction due to the Earth rotation.[4] The station clock runs slower when the Earth rotation adds to the Earth orbiting velocity and runs faster when the Earth rotation opposes the Earth orbital velocity. The moon and nearby planets also introduce relativistic time-keeping effects. The variation in the clock calibration due to the Earth rotation can be modeled as

$$F_e = a_e r_s \sin(\omega_e t + \lambda_s + \theta_{rc}) \tag{19}$$

A typical nominal value for the amplitude is given by $a_e = 3.17679 \times 10^{-10}$ s/km.

If an error for a_e is introduced into the model given by Eq. (19), the sensitivity to that error is given by

$$\Delta Z = C_3 f_t \frac{\partial^3 F}{\partial a_e \partial t^2} \Delta t_{\mathrm{rtlt}} \Delta a_e$$

$$= C_3 f_t \Delta t_{\mathrm{rtlt}} r_s \omega_e^2 \sin(\omega_e t + \lambda_s + \phi) \Delta_{a_e} \tag{20}$$

Figure 5 displays the residual signature due to a 100% error in the nominal value for a_e, with the signature model from Eq. (20).

Troposphere Error Signature

One of the most difficult effects to model is the media delay due to the Earth troposphere. Models of the troposphere delay include contributions due to a wet component (water vapor) and a dry component (other gases). Most of the variability is associated with the wet component that is empirically modeled[5,6] as

$$G_w = \frac{z_w}{\sin\gamma + [A_w/(B_w + \tan\gamma)]} \tag{21}$$

where z_w is the height of the wet troposphere at zenith (directly overhead), γ is the elevation angle of the Doppler signal, and A_w and B_w are parameters provided to model the bending at low-elevation angles,

$$\sin\gamma = \cos\delta \cos\lambda \cos\phi_s + \sin\phi_s \sin\delta \tag{22}$$

Definitions of λ, δ, and ϕ_s are found in Fig. 3. For small values of γ,

$$G_w \approx (1/c)(z_w/\sin\gamma) \tag{23}$$

If the random variation in the wet z height is modeled as a sinusoid

$$z_w = z_{w_0} + z_{w_1} \sin\left(\omega_{w_1} t\right) \tag{24}$$

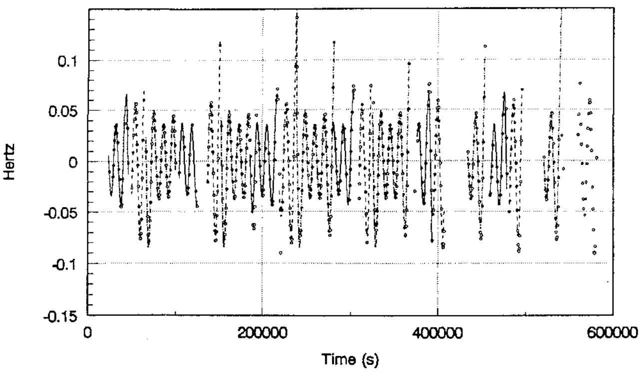

Fig. 6 Troposphere residuals with signature model.

then from Eq. (13) the residual signature introduced by an error in the amplitude z_{w_1} is given by

$$\Delta Z_{z_1} \approx \frac{2C_3 f_t}{c}\frac{\partial^2 G_w}{\partial z_1 \partial t}\Delta z_1$$

$$\approx \frac{2C_3 f_t}{c}\left\{\frac{1}{\sin\gamma}\omega_{w_1}\cos\omega_{w_1}t - \frac{\cos\gamma\dot{\gamma}}{\sin^2\gamma}\sin\omega_{w_1}t\right\}\Delta z_1 \tag{25}$$

where

$$\dot{\gamma} = \frac{\cos\phi(\cos\lambda - \cos\delta\sin\lambda)}{\cos\gamma}\dot{\lambda} \tag{26}$$

Figure 6 displays actual residuals when such an error is introduced into the troposphere model and the analytical match yielded by Eqs. (25) and (26).

Postfit Residuals

Postfit residuals are based on the estimates resulting from the orbit determination filtering process. Spacecraft position errors corresponding to each of the postfit residual cases are given in Table 2. The estimates of the spacecraft state based on the short data arc of 9000 s from the Mars Observer mission are referenced to the solution corresponding to a long data arc spanning several weeks that is assumed to represent the true spacecraft state.

The baseline case represents the best estimate of the spacecraft state after processing 9000 s of Doppler data using the most accurate models available. The displacement of the state estimate, computed from the components given in the table, is approximately 30 km from the assumed reference position. This small displacement may be attributed to data noise and unknown modeling errors. The postfit residuals for the baseline case are shown in Fig. 7. They follow the zero line; this is not a direct indication that the estimates are accurate but, rather, that they are a good fit to the assumed orbit determination model.

The introduction of a systematic error in the solar pressure model results in prefit residual errors shown in Fig. 2. After a new solution is obtained, the spacecraft state estimate is essentially the same as for the baseline case, as shown in Table 2. The postfit residual plot is virtually identical to that of the baseline case shown in Fig. 7. This result indicates that the solar pressure systematic error has been absorbed by other estimated parameters. The most likely candidate is the Mars ephemeris.

Systematic errors in station location and the relativistic clock model result in substantial spacecraft orbit estimate errors of up to 400 km. The postfit residual plots, however, are almost identical to the baseline postfit residuals, displaying little or no evidence of the errors. Figure 8 shows the postfit residuals for the case of a systematic clock error. These cases demonstrate the well-known result that postfit residual analysis alone is not sufficient. The orbit determination analyst must be aware that systematic errors may not appear in the postfit residual plot.

A similar analysis was performed to determine the effect of a systematic error in the troposphere model. For this case the spacecraft position error is about 100 km. The postfit residuals shown in Fig. 9 follow the prefit residual plot in Fig. 6. This type of error is not masked by the orbit determination process.

Table 2 Spacecraft state position errors, km

	X	Y	Z
Baseline	−9.1	−28.1	−3.0
Solar pressure	−9.1	−28.3	−2.9
Station location	−12.2	−160.0	405.0
Clock error	9.5	−77.0	131.9
Troposphere	25.8	0.7	−114.5

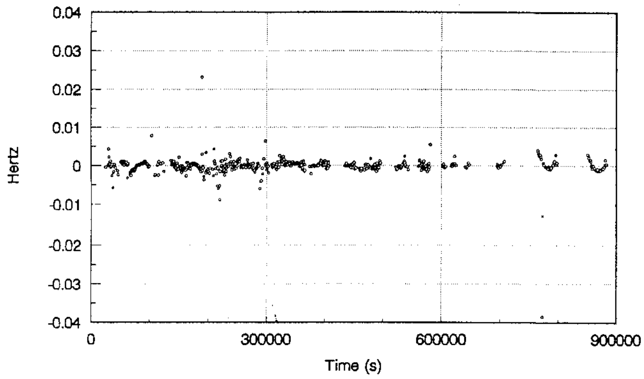

Fig. 7 Baseline postfit residuals.

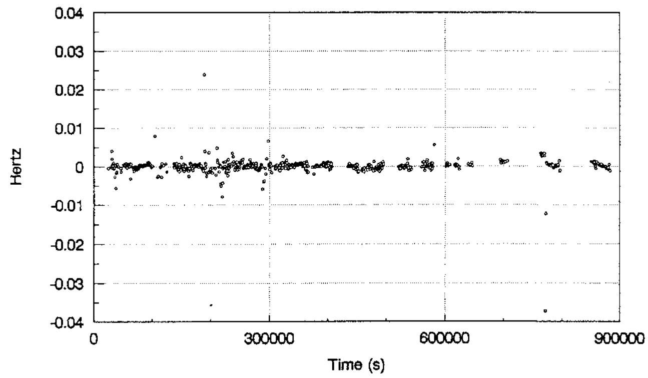

Fig. 8 Clock calibration postfit residuals.

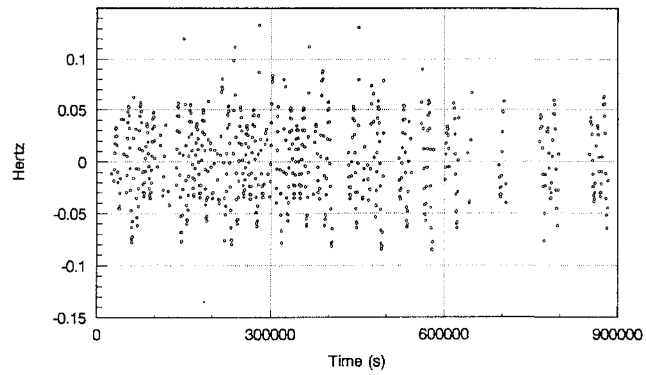

Fig. 9 Troposphere postfit residuals.

Conclusions

A procedure has been described for analytically characterizing Doppler residual signatures resulting from errors in model parameters. This method may provide a valuable diagnostic tool in analyzing prefit and postfit residuals. A comparison of postfit residuals with and without the introduction of known modeling errors, however, demonstrates that some errors can be masked by apparent convergence, resulting in erroneous estimates.

Acknowledgments

Accomplished with the support of NASA/JOVE Grant NAG 8-275. This research was presented as Paper 94-178 at the AAS/AIAA Spaceflight Mechanics Meeting, Cocoa Beach, FL, Feb. 16, 1993.

References

[1]Miller, J. K., "The Effect of Clock, Media, and Station Location Errors on Doppler Measurement Accuracy," *The Telecommunications and Data Acquisition Progress Report 42-113 January–March 1993*, Jet Propulsion Lab., California Inst. of Technology, Pasadena, CA, 1993, pp. 7–18.

[2]Moyer, T. D., "Mathematical Formulation of the Double-Precision Orbit Precision Program (DPODP)," Jet Propulsion Lab., California Inst. of Technology, JPL TR 32-1527, Pasadena, CA, May 1991.

[3]Hamilton, T. W., and Melbourne, W. G., "Information Content of a Single Pass of Doppler Data from a Distant Spacecraft," *Deep Space Network Space Program Summary 37-39*, Vol. 3, Jet Propulsion Lab., California Inst. of Technology, Pasadena, CA, 1966, pp. 18–23.

[4]Hellings, R. W., "Relativistic Effects in Astronomical Timing Measurements," *Astronomical Journal*, Vol. 91, No. 3, 1986.

[5]Chao, C. C., "New Tropospheric Range Corrections with Seasonal Adjustment," *Deep Space Network Progress Report*, Vol. 6, Jet Propulsion Lab., California Inst. of Technology, No. 32-1526, Pasadena, CA, 1971, pp. 67–73.

[6]Chao, C. C., "A New Method to Predict Wet Zenith Range Correction from Surface Measurements," *Deep Space Network Progress Report*, Vol. 14, Jet Propulsion Lab., California Inst. of Technology, No. 32-1526, Pasadena, CA, 1973, pp. 33–41.